Supporting Information

Pyridine-based Benzoquinone Derivatives as Organic Cathode Materials for Sodium Ion Batteries

Xiaoxue Li[a], Kangkang Jia[a], Jingwei Zhang[a], Xiaorui Liu[c], Lu Li[*b], Linna Zhu[*a], Fei Wu[*a]

[a] *Chongqing Key Laboratory for Advanced Materials and Technologies of Clean Energy, School of Materials & Energy, Southwest University Chongqing 400715, P. R. China.*

[b] *Chongqing University Key Laboratory of Micro/Nano Materials Engineering and Technology, Chongqing University of Arts and Sciences, Yongchuan, Chongqing, 402160, P. R. China.*

[c] *Key Laboratory of Luminescence Analysis and Molecular Sensing, Ministry of Education, School of Chemistry and Chemical Engineering, Southwest University, Chongqing 400715, P. R. China.*

E-mail: feiwu610@swu.edu.cn; lnzhu@swu.edu.cn.

Table of contents

1. General methods

All raw materials were purchased from commercial suppliers (Sigma Aldrich, and the Energy Chemical) and used without further purification if not mentioned otherwise. The nuclear magnetic resonance (NMR) spectra were obtained from a BRUKER AVANCEIII 600 MHz NMR Instrument (in $CDCl_3$). Data for ^1H NMR was recorded as follows: chemical shift (ppm), multiplicity (s, singlet; d, doublet; t, triplet; q, quarter; m, multiple), coupling constant (Hz), integration. Data for ^{13}C NMR was reported in terms of chemical shift (δ, ppm). JSM-7800F field emission scanning electron microscope was used to characterize morphology. The Fourier transform infrared spectrometer (FT-IR) was recorded using KBr pellets on a Thermo Nicolet 6700 with the wavenumber range of 400-4000 cm^{-1}. The X-ray photoelectron spectroscopy (XPS) was utilized to evaluate the surface compositions of the samples with model of thermo scientific K-Alpha. UV-Vis absorption spectra was collected on SPEC ORD 2010 plus Analytikjena.

2. Experimental section

Synthesis of 1,4-bis (2,6-dimethoxyphenyl) pyridine (QQPQ-1).

QQPQ-1 was synthesis by Suzuki cross-coupling reaction in an oven-dried 100 mL glass Schleck round-bottom flask equipped with a reflux condenser and a magnetic stirring bar under Ar_2 atmosphere. 2 g 2,6-dimethoxyphenylboronic acid and 3.69 g 2,6-dibromopyridine, 9.63 g Cs_2CO_3 and 1.38 g $Pd(PPh_3)_4$ were added into glass Schlenk round-bottom flask mentioned above in N_2, after that, 70 mL THF and 12 mL deionized water were added into the flask with a syringe. The mixture was heated to mild reflux

at an oil bath temperature of about 70 °C for 24 hours. The product was extracted using DCM and pure product was obtained through purifying the crude over silica gel using petroleum ether: ethyl acetate (5:1), and the QQPQ-1 was obtained as yellow solid, 2.55 g, 86% yield. ^{1}H NMR (600 MHz, $CDCl_3$) δ 7.81 (d, J = 7.7 Hz, 2H), 7.72 (t, J = 7.7 Hz, 1H), 7.56 (d, J = 2.8 Hz, 2H), 6.92 (dt, J = 8.9, 5.9 Hz, 4H), 3.83 (d, J = 1.9 Hz, 12H). ^{13}C NMR (151 MHz, $CDCl_3$) δ 155.05 (s), 154.01 (s), 151.60 (s), 135.42 (s), 130.32 (s), 123.21 (s), 116.41 (s), 115.28 (s), 113.28 (s), 56.54 (s), 55.84 (s).

Synthesis of 2,6-bis(p-benzoquinonyl) pyridine (QPQ-1).

0.5g QQPQ-1 was added into a 50mL round bottom flask equipped with a magnetic stirring bar, and 15mL acetonitrile solution was added to dissolve the solid, then the solution was cooled to 0 ºC. After that, 2.34g ceric ammonium nitrate (CAN, $Ce(NH4)_2(NO_3)_6$) was dissolved in 10 mL water and added into the solution drop by drop using a dropper. the solution became brown and solid appeared. Then the temperature is increased to room temperature and the solution stirred for 12h, the precipitated solid was washed over with water for 5 times. The crude product was obtained by recrystallization from 1,1,2,2-tetrachloroethane, and QPQ-1 was obtained as brown solid, 0.19 g, 45% yield. IR (KBr) ν_{max}: 1492, 1580, 1641, 2927 cm^{-1}.

Synthesis of 1,4-bis (2,5-dimethoxyphenyl) pyridine (QQPQ-2).

The synthesis of QQPQ-2 was similar to that of QQPQ-1. The feeding of 2,5-dimethoxyphenylboronic acid, 2,5-dibromopyridine, cesium carbonate and tetrakis(triphenylphosphine)palladium were 3.55 g (19.5 mmol, 2.4 eqv.), 2.00 g (8.13 mmol, 1.0 eqv.), 3.93 g (28.5 mmol, 3.5 eqv.), and 0.75 g (0.650 mmol, 0.08 eqv.),

respectively. The pure product was obtained through purifying the crude over silica gel using petroleum ether: ethyl acetate (3:2) as white solid, 1.49 g, 90% yield. ^{1}H NMR (600 MHz, $CDCl_3$) δ 8.86 (s, 1H), 7.90 (d, J = 5.2 Hz, 2H), 7.46 (d, J = 2.5 Hz, 1H), 7.03 – 6.92 (m, 4H), 3.83 (dd, J = 19.5, 12.3 Hz, 12H). ^{13}C NMR (151 MHz, $CDCl_3$) δ 154.20 – 153.86 (m), 151.50 (s), 151.05 (s), 149.70 (s), 136.47 (s), 132.09 (s), 129.66 (s), 128.09 (s), 124.27 (s), 115.77 (d, J = 17.5 Hz), 113.87 (s), 113.19 (s), 112.74 (s), 56.44 (s), 56.28 (s), 55.88 (d, J = 7.0 Hz).

Synthesis of 2,5-bis(p-benzoquinonyl) pyridine (QPQ-2).

The synthesis procedure of QPQ-2 was also similar to that of QPQ-1. The crude product was obtained by recrystallization from 1,1,2,2-tetrachloroethane as brown solid, 0.18 g, 42% yield. IR (KBr) ν_{max}: 1580, 1496, 2961, 1643 cm^{-1}.

3. Ex-situ characterization

The electrode sheets at different charging and discharging state were taken out from the batteries in a glove box filled with N_2 (O_2 and H_2O content < 0.1 ppm), and then washed with DOL/DME (v:v=1:1) to remove the residual electrolyte. Next, the electrodes were dried in vacuum environment for 2 hours, 60°C. After that, the electrodes were marked and stored in N_2-filled glove box. The samples were exposed in air when Ex-situ FTIR test conducted, and they were tested using the ATR pattern. For ex-situ XPS tests, the samples were prepared in a stream of Ar-flow, and then the ex-situ XPS measurement was carried out.

4. Electrochemical measurements

QPQ-1 and QPQ-2 electrodes were prepared through mixing active material

(QPQ-1/QPQ-2, 70 wt.%), conductive carbon materials (Graphene (GE), 20 wt.%) and 10 wt.% PVDF (polyvinylidene fluoride). The active molecules were first dissolved in N, N-dimethylformamide (DMF) and then Graphene was added into the solution, the mixture through ultrasonicating for one hour. After that, the solvent volatilizes completely by stirring and heating in the fume hood. PVDF and N-methyl-2-pyrrolidone (NMP) were added to fabricate a slurry. After that, the slurry was casted on Al foil current collector and dried at 60℃ for 12 h under vacuum. The pure GE electrode was made up of 90 wt.% GE and 10 wt.% PVDF binder. The electrochemical performance was test using CR2032-type coin cells, which were assembled in a glovebox filled with highly pure argon (oxygen and water content < 0.1 ppm). The electrolyte used in the batteries was 2 M sodium bis(trifluoromethanesulfonyl)imide (NaTFSI) in 1,3-dioxolane6 (DOL) and 1,2-dimethoxyethane (DME) (1/1, v/v), 120 μL for each coin was used. For the full cell, the anode was commercial hard carbon (CARBOTRON P(J)). Both anode and cathode were pre-sodiated for 3 cycles at a rate of 0.2C, and the specific capacity of full cell was depended on the mass of the cathode only. Conduct constant current charge and discharge test on the assembled battery through NEWARE battery test system (ct-4008t) between 1.0 and 3.6 V. The capacities were calculated based on the mass of active materials. Cyclic voltammetry (CV) and AC impedance (EIS) tests were obtained by Shanghai Chenhua 760e electrochemical workstation. The sweep speed of CV test was 0.1 mV s^{-1} and the voltage range was 1.0-3.6 V (vs. Na^+ / Na). The EIS test is conducted in the frequency range of 5 mV, 10^{-2}-10^5 Hz. All tests were performed at room temperature.

5. Supplementary Figures and Tables

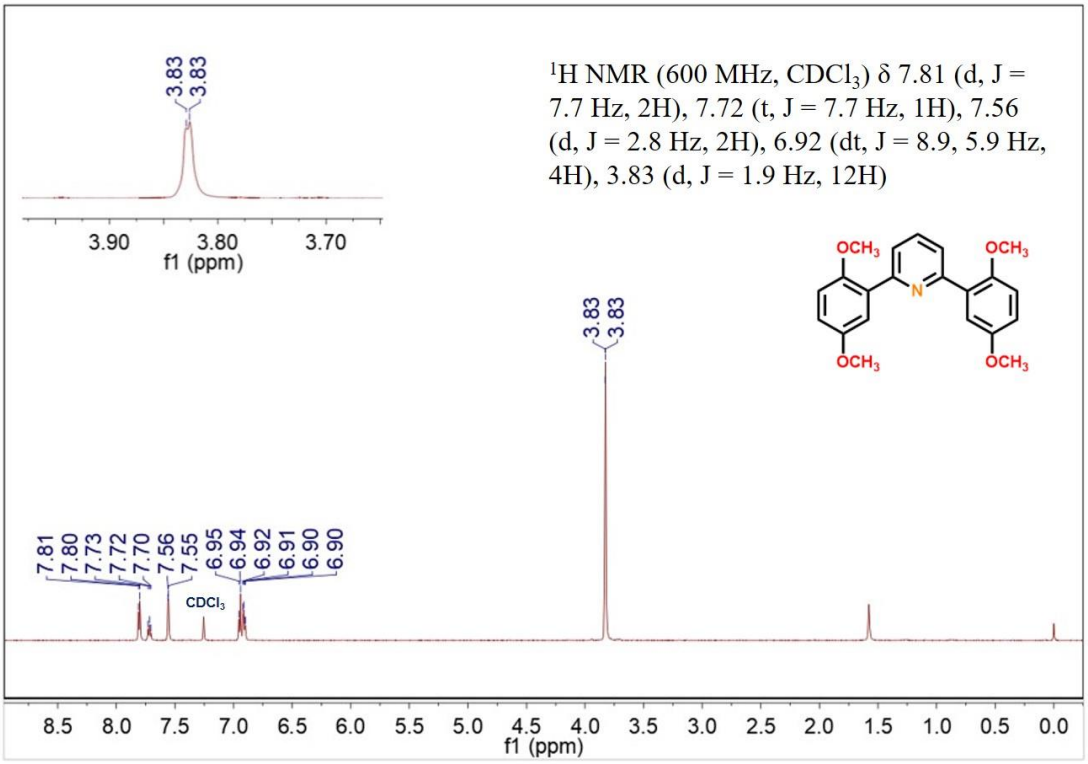

Figure S1. ^{1}H NMR (600 MHz, $CDCl_3$ solvent, 25°C) spectrum of QQPQ-1.

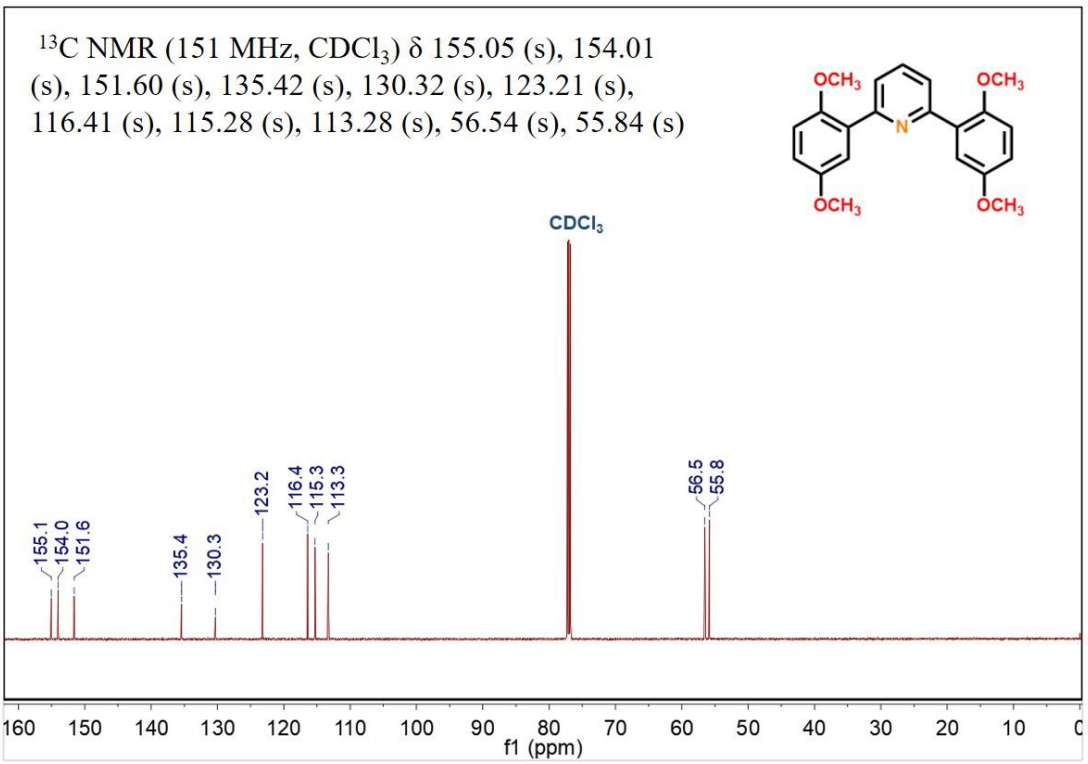

Figure S2. ^{13}C NMR (151 MHz, $CDCl_3$ solvent, 25°C) spectrum of QQPQ-1.

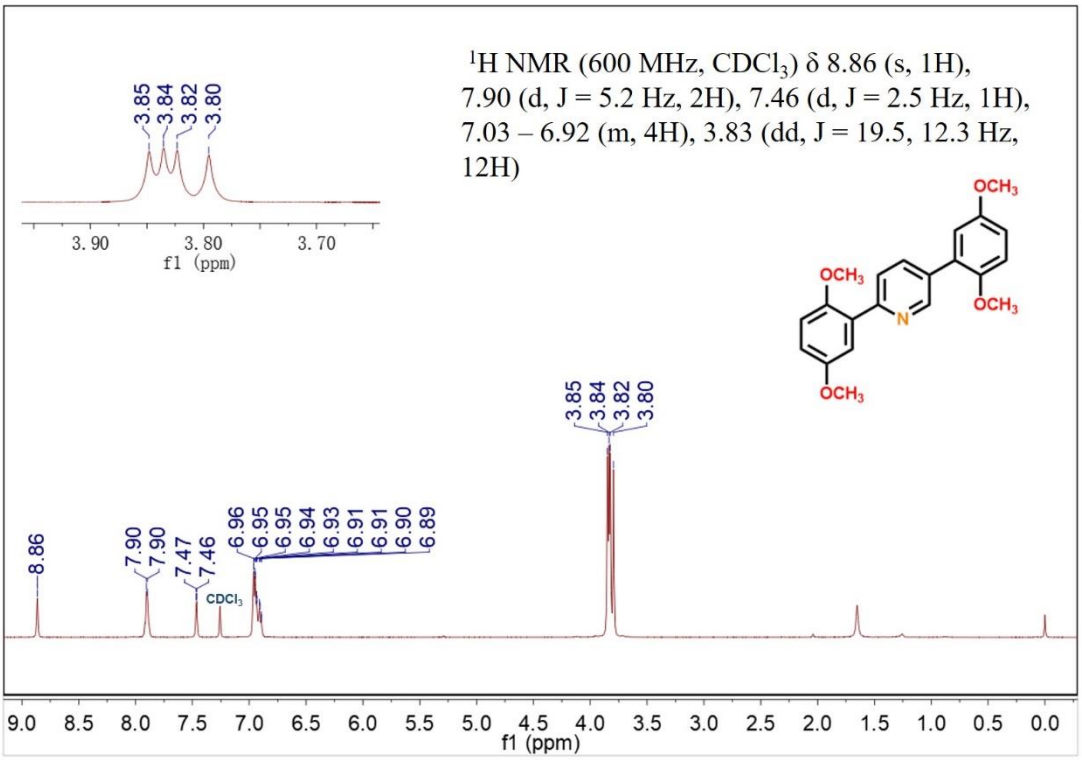

Figure S3. ^{1}H NMR (600 MHz, $CDCl_3$ solvent, 25°C) spectrum of QQPQ-2.

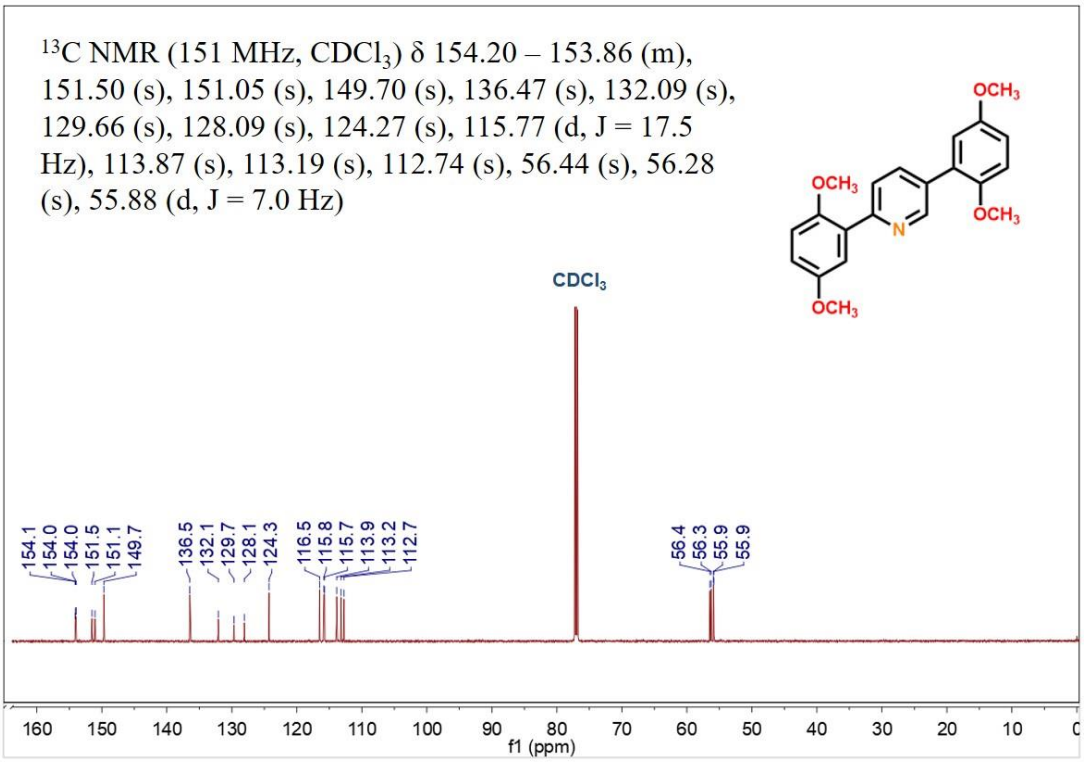

Figure S4. ^{13}C NMR (151 MHz, $CDCl_3$ solvent, 25°C) spectrum of QQPQ-2.

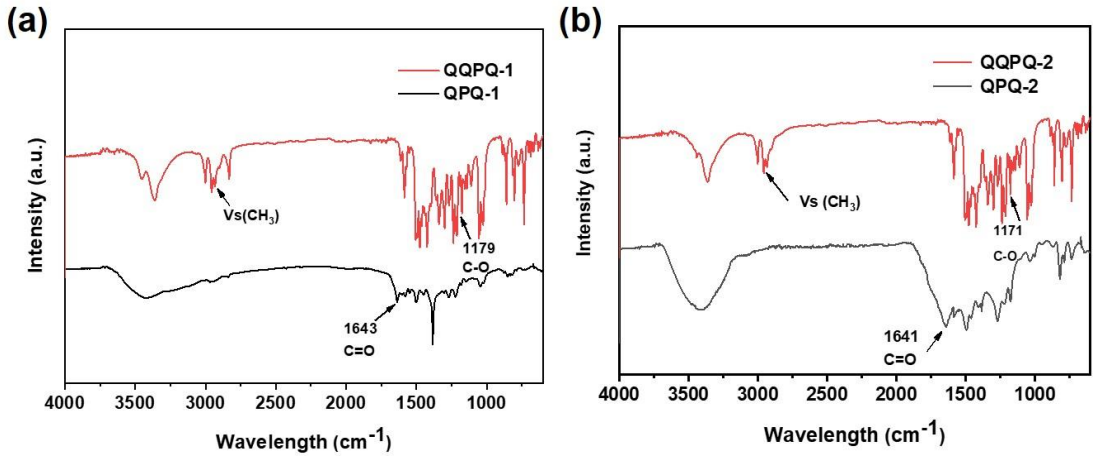

Figure S5. FTIR spectra (powder, 25°C) of (a) QQPQ-1, QPQ-1 and (b) QQPQ-2, QPQ-2.

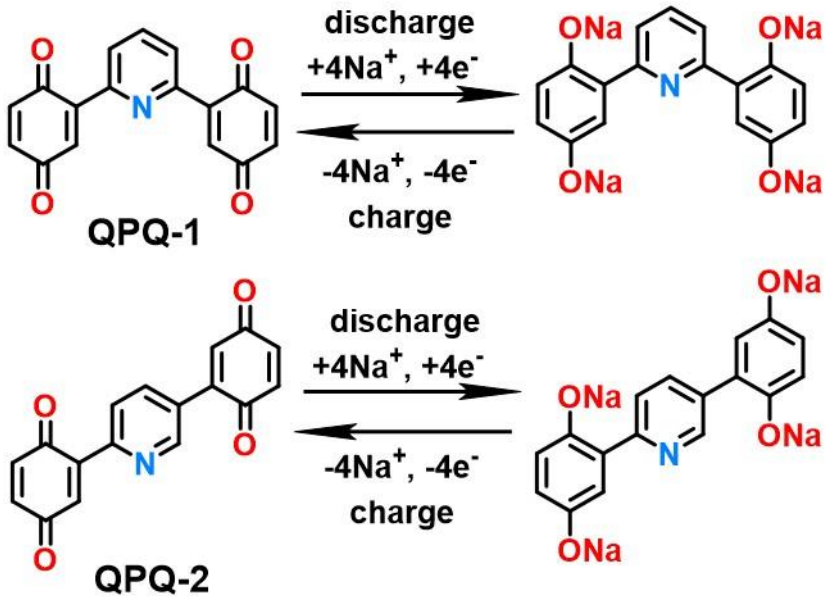

Figure S6. Proposed reaction mechanisms for QPQ-1 and QPQ-2 cathodes.

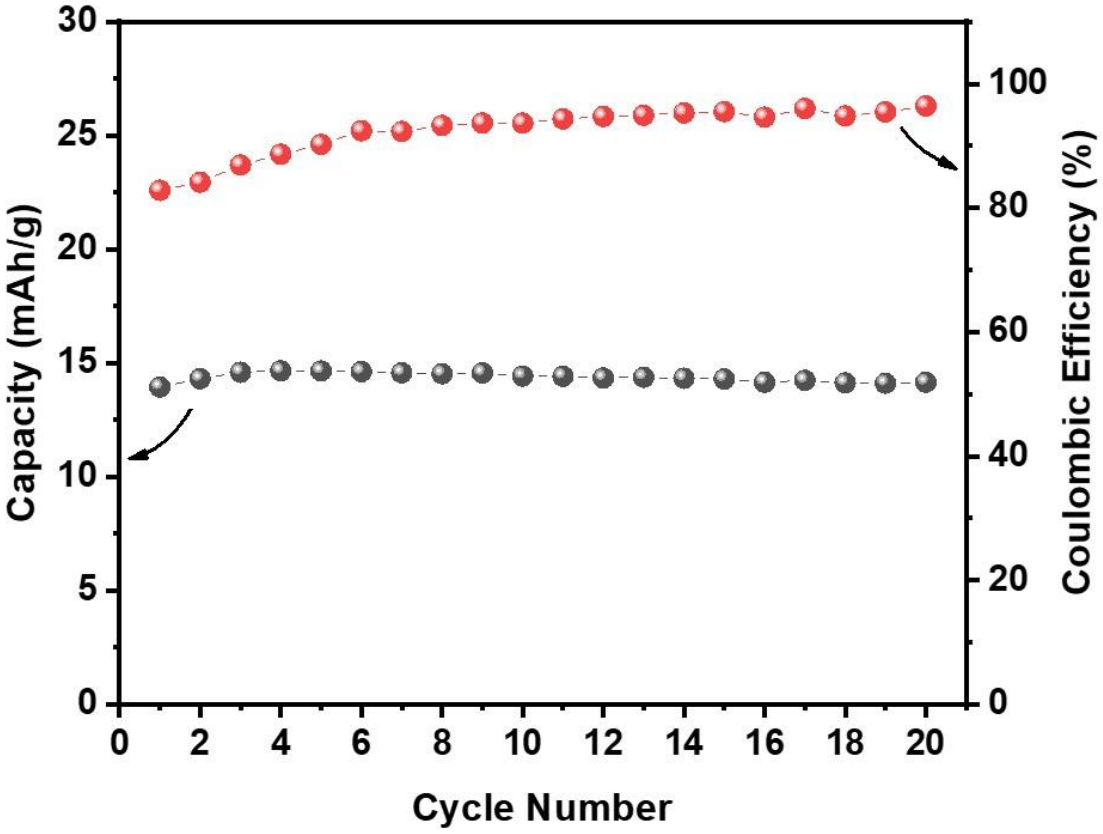

Figure S7. Cycling performance and Coulombic efficiency for Graphene.

Figure S8. The equivalent circuits of EIS data for QPQ-1 and QPQ-2 in Na-ion batteries

Table S1. Performances comparison between our cathode and some reported organic cathode materials for SIBs.

Materials	**Current density**	**Cycle number**	**Specific capacity (mAh/g)**	**Capacity retention (%)**	**Voltage plateau (V vs. Na^+/Na)**	**Reference**
AQ26ONa	50 mA/ g	50	142	70	1.0/1.5	[1]
PTCDI-DAQ	100 mA/g	200	206	94	2.1/2.6	[2]
PTCDA	200 mA/g	100	100	83	2.5/2.2	[3]
C4Q	0.1C	100	441	66	2.45/3.20	[4]
PLP-DAAQ (1,4)	50 mA/g	150	163	88	2.2/2.1/2.0	[5]
o-Na_2TBQ	50 mA/g	200	175	61	2.22/2.46	[6]
BAQIT	0.1C	90	200	65	1.5/1.9	[7]
PDBM	30 mA/g	100	210	57.6	3.0/3.3 V	[8]
PP-DAAQ (1,5)	50 mA/g	150	142	81.6	1.35/1.8/1.9	[9]
Na_2PDHBQS	100 mA/g	150	183	/	1.5	[10]
QPQ-2	**0.1 C**	**100**	**214**	**93**	**2.22/2.71**	**This work**

Table S2. Summary of R_s, R_f and R_{ct} (Ω) of QPQ-1 and QPQ-2 at different cycles.

	cycle	R_s (Ω)	R_f (Ω)	R_{ct} (Ω)
QPQ-1	pristine	22.09	47.21	419.37
	cycle 1	21.87	39.77	410.96
	cycle 10	22.97	44.85	500.89
QPQ-2	pristine	19.74	44.66	412.45
	cycle 1	20.89	38.73	407.66
	cycle 10	22.42	36.24	414.87

6. Computational details

Geometric structures and electronic properties of the investigated systems were fully optimized using B3LYP at 6-31G (d, p) levels.[11] The energies of all of the obtained geometries are ensured to be the lowest because the optimized structures do not exhibit imaginary frequency. A parameter of solvation free energy (ΔG) could be used to evaluate the solubility of an organic materials theoretically.[12] ΔG can be defined as the difference of free energy for the organic materials in solvent and gap.[13] Diethylether and 1,4-dioxane were selected in this works. The calculations of ground-state geometry and energy on DFT and TD-DFT were carried out by the Gaussian 09 program.[14]

Table S3. Calculated Solvation free energy (ΔG in kcal mol^{-1}) of QPQ-1 and QPQ-2.

	$\Delta G_{(diethylether)}$ /kcal mol^{-1}	$\Delta G_{(1,4\text{-dioxane})}$ /kcal mol^{-1}
QPQ-1	-4.50	-2.27
QPQ-2	-5.89	-3.79

Reference

[1] Jiahui Hu, Ren Liang, Wu Tang, Hengyang He, Cong Fan, Synthesis of polyanionic anthraquinones as new insoluble organic cathodes for organic Na-ion batteries, International Journal of Hydrogen Energy, 2020, 45, 24573−24581.

[2] Yang Hu, Qihang Yu, Wu Tang, Maozeng Cheng, Xinxin Wang, Sihong Liu, Jian Gao, Ming Wang, Ming Xiong, Jiahui Hu, Changyu Liu, Taotao Zou, Cong Fan, Ultra-stable, ultra-long-lifespan and ultra-high-rate Na-ion batteries using small-molecule organic cathodes, Energy Storage Materials, 2021, 41, 738–747.

[3] Chenpei Yuan, Qiong Wu, Qi Shao Qiang Li, Bo Gao, Qian Duan, Hengguo Wang, Free-standing and flexible organic cathode based on aromatic carbonyl compound/carbon nanotube composite for lithium and sodium organic batteries, J. Colloid Interface Sci, 2018, 517, 72−79.

[4] Bing Yan, Lijiang Wang, Weiwei Huang, Shibing Zheng, Pandeng Hu and Yuyu Du, High-capacity organic sodium ion batteries using a sustainable C4Q/CMK-3/SWCNT electrode, Inorg. Chem. Front., 2019, 6, 1977–1985.

[5] Fei Xu, Hongtao Wang, Jianghui Lin, Xiao Luo, Shun-an Cao and Hanxi Yang, Poly (anthraquinonyl imide) as a high capacity organic cathode material for Na-ion batteries, J. Mater. Chem. A, 2016, 4, 11491−11497.

[6] Li-Min Zhu, Guo-Chun Ding, Qing Han, Yong-Xia Miao, Xin Li, Xin-Li Yang, Lei Chen, Gong-Ke Wang, Ling-Ling Xie & Xiao-Yu Cao, Enhancing electrochemical performances of small quinone toward lithium and sodium energy storage, Rare Met, 2022, 41, 425–437.

[7] Dylan Wilkinson, Manik Bhosale, Marco Amores, Gollapally Naresh, Serena A. Cussen, and Graeme Cooke, A Quinone-Based Cathode Material for High-Performance Organic Lithium and Sodium Batteries, 2021, 4, 12084-12090.

[8] Limin Zhu, Guochun Ding, Jingbo Liu, Ziqi Liu, Lingling Xie, Xiaoyu Cao, Graphene-wrapped poly(2,5-dihydroxy-1,4-benzoquinone-3,6-methylene) nanoflowers as low-cost and high-performance cathode materials for sodium-ion batteries, Int J Energy Res, 2019, 43:7635–7645.

[9] Fei Xu, Hongtao Wang, Jianghui Lin, Xiao Luo, Shun-an Cao and Hanxi Yang, Poly(anthraquinonyl imide) as a high capacity organic cathode material for Na-ion batteries, 2016, 4, 11491-11497.

[10] Aihua Li, Zhenyu Feng, Yan Sun, Limei Shang, Liqiang Xu, Porous organic polymer/RGO composite as high performance cathode for half and full sodium ion batteries, J. Power Sources, 2017, 343, 424−430.

[11] A. Cohen, P. Mori-Sánchez and W. Yang, Challenges for density functional theory, Chem. Rev., 2012, 112, 289-320.

[12] J. M. Ho, A. Klamt and M. L. Coote, Comment on the correct use of continuum solvent models, J Phys Chem A, 2010, 114, 13442-13444.

[13] Y. Zhang, Y. Y. Li, C. Chen, L. Wang and J. L. Zhang, Design new hole transport materials for efficient perovskite solar cells by suitable combination of donor and core groups, Organic Electronics, 2017, 49, 255-261.

[14] M. J. Frisch, G. W. Trucks, H. B. Schlegel, G. E. Scuseria, M. A. Robb, J. R. Cheeseman, G. Scalmani, V. Barone and G. A. Petersson, “Gaussian 09” Revision A. 1,

Gaussian, Inc, Wallingford, 2009.